The NLRP3 inflammasome signaling axis plays a primary role in acrylamide-induced pyroptosis and neurotoxic injury in SH-SY5Y cells

Mengyao Zhao
East China University of Science and Technology
Boya Zhang
East China University of Science and Technology
Linlin Deng
East China University of Science and Technology
Liming Zhao (zhaoliming@ecust.edu.cn)
East China University of Science and Technology https://orcid.org/0000-0002-8523-103X

Research Article

Keywords: Acrylamide, Pyroptosis, NLRP3 inflammasome, Neuroinflammation

Posted Date: April 22nd, 2022

DOI: https://doi.org/10.21203/rs.3.rs-1562240/v1

Abstract

Acrylamide (ACR), a soft electrophile, is a typical environmental and food contaminant that presents potential health hazards and, consequently, is attracting increasing attention in the quest for its control. ACR neurotoxicity has been widely reported in experimental animals and attributed to neuroinflammation, however the mechanisms involved therein require clarification. In this study, we used a neuron cell model to investigate the mechanisms of ACR-induced neuroinflammation and pyroptosis. The results showed that ACR treatment induced lytic cell death morphologically under both the canonical pyroptotic pathway (NOD-like receptor protein 3 (NLRP3)-apoptosis-associated speck-like protein containing CARD (ASC)-cysteinyl aspartate specific proteinase 1 (caspase-1) -gasdermin D (GSDMD) -interleukin-1β (IL-1β)/interleukin-18 (IL-18)) and an alternative pyroptotic pathway (Cysteinyl aspartate specific proteinase 3 (caspase-3) -gasdermin E (GSDME) -IL-1β/IL-18) in SH-SY5Y cells. Moreover, the lactate dehydrogenase (LDH) production, cytokines release and lytic cell death induced by ACR were diminished by caspase-1 and -3 inhibitors. Furthermore, the knockdown of caspase-1 by small interfering RNA attenuated ACR-induced lytic cell death, suggesting that canonical pyroptosis (the NLRP3-caspase 1-GSDMD-IL-1β signaling axis) played a primary role in the ACR-induced pyroptosis. Of the two pyroptotic-related pathways, the NLRP3 inflammasome cascade was activated first within the 6 h period of ACR exposure, while the activation of the alternative pyroptotic pathway was delayed. Collectively, these results indicate that ACR mainly induce NLRP3-related neuroinflammation and pyroptosis in SH-SY5Y cells, which is, thus, suggestive of an alternative mechanism for ACR-induced neurotoxicity.

Introduction

Acrylamide (ACR) has attracted extensive attention due to its potential impact on environment and human health via daily exposure. ACR has been scientifically confirmed to cause neurotoxicity, genotoxicity, developmental toxicity and potential carcinogenicity to both humans and animals, thus raising widespread concern [1–3]. Consequently, several investigations have fueled advances in various underlying mechanisms through which to address ACR-induced neurotoxicity. These include the axonal degeneration of the nervous system [4,5]; the alteration of neurotransmitter levels and inhibition of neurotransmission [6,1]; nerve cell apoptosis [7–9]; oxidative stress and disruption in ion homeostasis [7,10,11]; as well as adduct formation with cytoskeletal proteins or deoxyribonucleic acid [5,12]. Several other studies have focused on the role of inflammation in the neurotoxicity caused by ACR [13,14], and a connection has been revealed between NLRP3 inflammasomes and ACR-induced neurotoxicity [15]. However, the specific regulatory role and mechanism of NLRP3 inflammasome in ACR-induced neurotoxicity require further clarification.

Canonical NLRP3 inflammasome is comprised of effector protein caspase-1, adaptor protein ASC, and sensory protein NLRP3 [16]. It requires priming and activation to become operational. The priming process includes pro-IL-18, pro-IL-1β, and NLRP3 expression, the initiation of which normally occurs via the signaling pathway of nuclear factor-kappa B [17,18]. Moreover, the activation process enables inflammasome complex assembly, facilitating pro-caspase-1 cleavage to obtain active caspase-1,

followed by the release of mature IL-18 and IL-1β via pro-IL-18 and pro-IL-1β cleavage [19]. Additionally, the GSDMD is released via the activated caspase-1 cleavage, forming pores in the plasma membrane to rapidly release mature IL-18 and IL-1β into the extracellular environment, which has been shown to cause neurocyte swelling in ACR-treated mice [20]. Neurocyte swelling, NLRP3 inflammasome activation and inflammatory factor release (mature IL-18 and IL-1β) are all typical features of pyroptosis [21]. However, the potential underlying mechanism between pyroptosis and ACR-induced neurotoxicity in neurocytes has not yet been comprehensively elucidated.

In addition to the canonical pathway, caspase-3 and GSDME can also facilitate the release of mature IL-18 and IL-1β and induce inflammatory cell death, a process known as alternative pyroptosis in many neurodegenerative diseases and inflammatory response models [22,23]. It remains unknown, however, whether the caspase-3-GSDME-IL-1β/IL-18 signaling axis contributes to ACR-induced pyroptosis and neurotoxicity. Furthermore, assuming both the canonical pyroptotic cascade and alternative pyroptotic cascade contribute to ACR-induced neurotoxicity, it is not clear which of these acts as the primary signal cascade (NLRP3-ASC-caspase-1-GSDMD-IL-1β/IL-18 or caspase-3-GSDME-IL-1β/IL-18), and their contributions to pyroptosis and neurological impact, thus, require further exploration.

As a dopaminergic neuron, SH-SY5Y cells are widely used in the study of neurodegenerative diseases such as Parkinson's and Alzheimer's, amongst others [24]. In this study, we established an in vitro SH-SY5Y cell model to clarify the role of the NLRP3 inflammasome-related canonical pyroptotic cascade and caspase 3-GSDME related alternative pyroptotic cascade in the mechanism of ACR-induced neurotoxicity. Furthermore, specific chemical inhibitors of caspase-1 and caspase-3 and small interfering (si)RNAs caspase-1 and caspase-3 were used to ascertain which signal pathway – either NLRP3 inflammasome cascade (caspase-1 enrolled) or caspase-3-GSDME cascade (caspase-3 enrolled) – plays the most significant role in ACR-induced pyroptosis and neurotoxicity. The sequential activation of these two pathways in SH-SY5Y cells was also investigated. It is hoped that the findings of this study will provide a new theoretical basis and novel research directions in the exploration of ACR-induced neurotoxicity.

Material And Methods

Materials

The Chinese Academy of Sciences (Shanghai, China) provided the human dopaminergic neuroblastoma SH-SY5Y cell line, while Gibco (Thermo Scientific, Shanghai, China) supplied the fetal bovine serum (FBS). Invitrogen (Thermo Scientific, Shanghai, China) supplied the Minimum Essential Medium (MEM), F12, GlutaMAX, sodium pyruvate, non-essential amino acid and penicillin/streptomycin. Antibodies against NLRP3 (1:1000; Proteinch; 00080435); ASC (1:1000; Proteinch; A16672); IL-1β (1:1000; ABclonal; A16288); IL-18 (1:1000; ABclonal; A16737); GSDMD/N-GSDMD (1:1000; Abcam; ab209845); GSDME/N-GSDME (1:1000; Abcam; ab215191); cleaved caspase-3 (1:1000; CST; 9664S), cleaved caspase-1 (1:1000; CST; 4199T) and β-actin (1:1000; CST; 4970S) were separately obtained from attached commercial company. Additionally, dimethyl sulfoxide (DMSO), 3-(4, 5-dimethyl-2-thiazolyl)-2, 5-diphenyl-

2-H-tetrazolium bromide (MTT), and N-Acetyl-L-cysteine (NAC) were acquired from Sigma-Aldrich (Shanghai, China). All related chemical agents were of analytical grade.

Cell culture

Human dopaminergic neuroblastoma SH-SY5Y cell lines were cultured in MEM/F12 medium supplemented with 10% FBS, 1% GlutaMAX, 1% sodium pyruvate, 1% non-essential amino acid, and 1% penicillin/streptomycin. A humidified incubator with air levels at 95% and a CO_2 level of 5% was used to cultivate the cells at 37°C. The growth medium was changed at intervals of 2 to 3 d.

Thereafter, the cells were placed into 96-, 24- or 6-well plates and left to incubate for 24–72 h. The existing media were then replaced with new media comprising varying concentrations of ACR and left to incubate for a further 24–72 h.

Cell viability

The viability of the cells was determined using MTT evaluation [25]. Briefly, a 96-well plate was used to seed SH-SY5Y cells at 8×10^3 cells per well, after which they were treated for 24 h, 48 h and 72 h, with different ACR concentrations of 0.01, 0.05, 0.1, 0.25, 0.5, 1.0, 2.5 and 5 mM each. Next, 10 μL of MTT (5 mg/mL) was added to each well and they were incubated for 2 h at 37°C. The media was replaced by 100 μL DMSO, after which a TECAN Infinite M200 PRO microplate reader was used to determine the absorbance at 570 nm. The control cell formazan density was regarded as 100%, while the cytotoxicities of the different groups were presented as proportions of the control group.

LDH assay and cell morphological examination

Cell pyroptosis was determined via LDH release using a CytoTox 96 cytotoxicity assay kit (Promega, Shanghai, China), according to the manufacturer's instructions. Briefly, the cells were seeded into a transparent 6-well plate. When the cells had grown approximately 80%, they were treated with ACR prepared with serum-free medium for 24 h. The cell supernatant was subsequently collected and transferred into a new 96-well plate and left to react for 30 min in the dark with the LDH detection working solution. The quantitative LDH levels were measured using a TECAN Infinite M200 PRO microplate reader (Tecan Trading AG, Switzerland) at 490 nm.

Cell morphology was observed using a Nikon Eclipse TI microscope (Nikon, Tokyo, Japan) at 100×/250× magnification. Briefly, cells were cultured in a 24-well plate at a density of 10^5 cells/well, after which they were treated for 24 h with different concentrations of ACR. Cellular ballooning was denoted with black arrows.

Measurement of reactive oxygen species (ROS), malondialdehyde (MDA), and glutathione (GSH) contents

For NAC treatment, the cells were pre-treated with 500 μM NAC for 1 h, and then co-treated with ACR for 24 h. A 2,7-dichlorofluorescin diacetate (DCFH-DA) staining kit (E004-1-1, Nanjing Jiancheng

Bioengineering Institute, Nanjing, China) was used to measure the ROS formation. Meanwhile, the cellular GSH (A006-2-1) and MDA (A003-1-2) concentrations were measured according to the directions of the supplier (Nanjing Jiancheng Bioengineering Institute, Nanjing, China). A bicinchoninic acid (BCA) protein assay kit (A045-4-2, provided by the Nanjing Jiancheng Bioengineering Institute, Nanjing, China) was used for cell lysis, employing an ultrasonic cell disruptor for protein concentration determination.

Western blot analysis

Radioimmunoprecipitation (RIPA) assay buffer (Beyotime, Shanghai, China) was used to extract cell pellets for 30 min, after which the lysates were subjected to centrifugation at 4°C for 10 min at 12,000 *g* to remove the insoluble substances. Thereafter, the protein was extracted from the supernatant and kept at 95°C for 5 min. The proteins (20–50 μg) were then separated using SDS-PAGE and moved to poly (vinylidene fluoride) (PVDF) membranes (GE Healthcare, IL, USA). The membranes were blocked with 5% fat-free milk (Sangon Biotech, Shanghai, China) or 5% bovine serum albumin (BSA) (Bio-Sharp, Hefei, China) for 1 h at room temperature, after which they were incubated overnight at 4°C with specific primary antibodies. The secondary HRP-conjugated antibodies were subsequently washed three times with tris-buffered saline with Tween 20 (TBST), then used to incubate the membranes at room temperature for 1 h. Protein detection was accomplished using an enhanced chemiluminescence (ECL) assay, obtained from Bio-Rad (Shanghai, China), while a Tanon 4200 imaging system (Tanon, Shanghai, China) was used for scanning.

ELISA assays

The expression levels of IL-1β, IL-18 and tumor necrosis factor-α (TNF-α) in the cell supernatant were measured using an ELISA kit (Elabscience, Houston, TX), according to the manufacturer's instructions. Briefly, 50 μL cell supernatant of each sample was added into a pre-coated 96-well microplate and left for 2 h at room temperature. The wells were then washed four times with the provided washing solution, biotinylated antibody was added and the cells were cultured at room temperature for 1 h. Thereafter, the washing process was repeated before HRP-streptavidin solution was added and the cells were then incubated at room temperature for 15–30 min, after which time a stop solution was added, and absorbance was measured at 450 nm immediately on a microplate reader.

Chemical inhibitor treatment

Doses of Ac-DEVD-CHO (Beyotime, Shanghai, China) and Ac-YVAD-CMK (Santa Cruz Biotechnology, Shanghai, China) were chosen via an MTT cell viability assay. For chemical inhibitor treatment, the SH-SY5Y cells were pre-treated for 24 h with either the Ac-DEVD-CHO or Ac-YVAD-CMK, and then treated either with or without ACR for 24 h. After the inhibition, the levels of LDH in the different treatment groups were measured in cell supernatant to check the inhibition efficiency.

Short interfering RNA (siRNA) silencing

The SH-SY5Y cells were transfected with a negative control siRNA (Santa Cruz Biotechnology, Shanghai, China) or caspase-1 siRNA/caspase-3 siRNA (Santa Cruz Biotechnology, Shanghai, China) using a

Lipofectamine 3000 Kit (Thermo Fisher Scientific, USA), according to the manufacturer's instructions. Briefly, cells were seeded onto 6-well plates and transfected with a mixture comprising the siRNA duplexes, Lipofectamine 3000, and Opti-MEM reduced serum medium (Gibco, USA). Following incubation for 48 h, the medium was replaced with a fresh cell cultural medium containing 10% FBS. Cells were then treated with either ACR or a vehicle (phosphate buffered saline (PBS)) and left for 24 h, after which they were harvested for LDH levels measurement and protein expression analyses.

Statistical analysis

Each assay was conducted at least in triplicate. Data was analyzed using the GraphPad Prism 7.0 software (GraphPad Software, La Jolla, CA), and the results were introduced as mean ± SD. Statistical comparisons between the experimental groups were evaluated by one-way analysis of variance (ANOVA) with Duncan's multiple comparison test using SPSS software v. 21. Consequently, $p < 0.05$ values were regarded as statistically significant and were denoted by different letters. Western blotting gray analysis was performed using the Image J imaging processing program (Wayne Rasband, National Institutes of Health, USA).

Results

ACR induced pyroptosis in SH-SY5Y cells

The SH-SY5Y cells were exposed to different concentrations of ACR for 24 h, 48 h and 72 h. The results are shown in Fig. 1A. Compared with the control group, the overall survival rate of the SH-SY5Y cells decreased as ACR concentrations increased and treatments were extended. The IC_{50} dose of ACR for 24 h was found to be 3 mM in the SH-SY5Y cells. Moreover, the effect of ACR on the morphology of SH-SY5Y cells can be seen in Fig. 1C. In the control group, the SH-SY5Y cells displayed a uniform cytoplasm, and a well-arranged structure with typical differentiation. However, following ACR treatment, the cells became round and floated, accompanied by obvious cellular ballooning (indicated by black arrow). These results suggest that ACR may induce pyroptosis in SH-SY5Y cells.

It is typical for pyroptosis to destroy the integrity of a cell membrane, leading to the release of LDH and cytokines into the extracellular environment [26]. As shown in Fig. 1B, with increased ACR concentration, the LDH levels in the SH-SY5Y cell supernatant increased significantly. A high dose of ACR for 24 h increased the LDH level in treated cells to 40 ± 3.18%, in comparison with the control group. As a defensive immune response [27], inflammation can trigger IL-1β, IL-18, TNF-α secretion significantly, which can lead to immune inflammation. In this study, the contents of cytokines like IL-18 and TNF-α in the supernatant were found to increase in a dose-dependent manner in line with the increase of ACR exposure and concentration, while the level of IL-1β also increased significantly, but was not dose dependent (Fig. 1D-F, $P < 0.05$).

ACR induced oxidative stress in SH-SY5Y cells

After the SH-SY5Y cells were treated with different concentrations of ACR for 24 h, remarkable markers of ROS were detected. As shown in Fig. 1G, compared with the control group, the levels of ROS in the SH-SY5Y cells had increased significantly (Fig. 1G, $P < 0.05$), however, protection with common antioxidant NAC was found to reduce the intracellular ROS accumulation ($P < 0.05$). At the same time, the level of GSH in the SH-SY5Y cells treated with ACR decreased significantly (Fig. 1H). In addition, compared with the control group, the MDA level in SH-SY5Y cells increased significantly after ACR treatment (Fig. 1I). Intracellular antioxidant GSH plays an important role in the elimination of ROS [28]. Thus, these findings demonstrate that ACR can significantly reduce the level of intracellular GSH and increase the level of MDA, suggesting that ACR can reduce the antioxidant capacity of cells and induce oxidative injury in SH-SY5Y cells.

ACR induced the expression of pyroptosis-related proteins in SH-SY5Y cells

With the cellular ballooning phenotype, we further investigated the related intracellular proteins expression by western blot. As expected, NLRP3-mediated pyroptosis was induced in this cell line upon the stimulation of ACR (Fig. 2A). Compared with the control group, the intracellular NLRP3, ASC, cleaved caspase-1 and N-GSDMD levels increased significantly, and in a dose-dependent manner, after ACR exposure (Fig. 2B-E, $P < 0.05$), indicating that ACR-induced oxidative stress could activate the NLRP3 inflammasome pathway, lead to the release of cytokines, and finally cause pyroptosis in SH-SY5Y cells.

In addition, apoptotic caspases (caspase-8/-3) were also seen to be activated (Fig. 2F and G, $P < 0.05$). In a pyroptotic-related signal cascade, caspase-3 can trigger GSDME activation and contribute to lytic cell death [29]. Meanwhile, our results showed that GSDME was cleaved in the ACR-exposed cells and the expression of N-GSDME increased significantly (Fig. 2H, $P < 0.05$), suggesting that caspase-3/GSDME may also be involved in the regulation of ACR-induced pyroptosis of SH-SY5Y cells. It is worth noting that both the canonical pyroptotic pathway (NLRP3/caspase-1/GSDMD) and the alternative pyroptotic pathway (caspase-8/caspase-3/GSDME) were involved in the pyroptosis of the SH-SY5Y cells induced by ACR. The order of these activations and the contributions of these two pathways to the neurotoxicity induced by ACR are, however, still unknown and require further investigation.

Canonical pyroptotic pathway and alternative pyroptotic pathway were sequentially activated by ACR

SH-SY5Y cells were treated with ACR for either 6 h or 24 h to observe the differences in cell phenotype and the expression of related proteins, so as to investigate whether the activation of the two pathways is sequential. The morphology of cells at different exposure periods were observed and the results are shown in Fig. 3A. Compared with the control group, after 6 h the ACR-infected cells were found to have decreased significantly in number, but with no obvious cellular ballooning. However, after 24 h ACR exposure, the number of cells had decreased further and the floating cells had increased significantly,

accompanied by a large extent of cellular ballooning (indicated by black arrows). Moreover, the integrity of cell membranes was investigated by measuring extracellular LDH levels. Compared with the control group, the level of LDH release had not increased significantly after 6 h ACR exposure ($P > 0.05$) but had increased significantly after 24 h ACR exposure (Fig. 3B, $P < 0.05$), suggesting that ACR time-dependently induced the pyroptosis of SH-SY5Y cells.

The expression levels of proteins in both the canonical pyroptotic and the alternative pyroptotic pathways were further investigated and the results showed that, compared with the control group, the protein levels of NLRP3 and cleaved caspase-1 increased significantly after 6 h of ACR exposure. Furthermore, N-GSDMD was found to have increased slightly, indicating that the NLRP3 inflammasome pathway in SH-SY5Y cells had begun within 6 h. After 24 h treatment, the expressions of related proteins in NLRP3 inflammasome pathway were enhanced (Fig. 4B-F, $P < 0.05$). However, after 6 h ACR treatment, only caspase-8 was activated and there was no significant change in other protein levels of the GSDME signaling axis, including cleaved caspase-3 and N-GSDME (Fig. 4G-J, $P > 0.05$), indicating that the effector proteins in the alternative pathway had not been fully activated. After 24 h of ACR exposure, however, the expression levels of cleaved caspase-8, cleaved caspase-3 and N-GSDME were found to have increased significantly (Fig. 4G, I and 4J, $P < 0.05$). These results suggest that prolonged treatment with ACR induced caspase-3/N-GSDME activation, while also enhancing NLRP3 inflammasome-mediated pyroptosis in the SH-SY5Y cells. Thus, ACR may first activate the NLRP3/caspase-1/GSDMD signaling axis by inducing cell oxidative stress, thereafter activating the caspase-8/caspase-3/GSDME signaling axis, and, consequently, contribute to pyroptosis in SH-SY5Y cells.

NLRP3 inflammasome signaling played a crucial role in ACR-induced pyroptosis in SH-SY5Y cells

In order to further clarify the mechanism underlying ACR-induced neurotoxicity, we further explored the pathways' key roles using the specific antagonist and siRNA gene silencing to prevent the specific signaling transduction.

SH-SY5Y cells were separately treated with different doses of the caspase-1 specific chemical inhibitor Ac-YVAD-CMK and caspase-3 specific chemical inhibitor Ac-DEVD-CHO for 24 h to select the appropriate dose (Fig. S1A and B). The caspase-1 inhibitor Ac-YVAD-CMK was found to markedly attenuate the LDH release induced by ACR to 7 ± 4.60%, while after treatment with the caspase-3 inhibitor Ac-DEVD-CHO treatment, the LDH release level was found to have decreased to 20 ± 2.86% (Fig. 5A). It is worth noting that, compared with the caspase-3 specific chemical inhibitor, the caspase-1 specific chemical inhibitor more effectively alleviated the release of LDH induced by ACR, indicating that the NLRP3-caspase 1-GSDMD signaling axis may play the primary role in ACR-induced pyroptosis. However, when the intervention of the two caspase proteins by these specific chemical inhibitors was simultaneous, the release of LDH levels decreased to 5 ± 5.54%, which is not significantly different from that of the control group (Fig. 5A). These results suggest that ACR-induced inflammatory response and pyroptosis in SH-SY5Y cells are attributed to the two pathways. Furthermore, caspase-1 and caspase-3 were knocked

down using a specific siRNA, and transfected cells were cultured for 24 h, either with or without ACR, to verify these signaling axes. Similar to the effects of the specific chemical inhibitors, siRNA-mediated caspase-1 and caspase-3 knock-down significantly alleviated the ACR-induced LDH release and cell lytic death (Fig. 5B). Following caspase-1 silencing, ACR-induced pyroptosis was found to be significantly reduced, and the release level of LDH was also significantly reduced to 15.71 ± 0.65% (Fig. 5B). Similarly, the silencing of caspase-3 effectively alleviated ACR-induced cytotoxicity in the SH-SY5Y cells, and the LDH release level decreased to 25.24 ± 1.35% (Fig. 5B). When caspase-1 and caspase-3 were silenced simultaneously, the LDH release level was further reduced to 10.31 ± 1.35% (Fig. 5B). These results further proved the involvement of caspase-1 and caspase-3 in the ACR-induced pyroptosis of SH-SY5Y cells. In light of the above comprehensive results, we further speculate that the NLRP3-caspase 1-GSDMD signaling axis may play a leading role in the pyroptosis of SH-SY5Y cells induced by ACR.

Caspase-1 siRNA silencing attenuated ACR-induced pyroptosis by reducing NLRP3 inflammasome protein expression in SH-SY5Y cells

Since the siRNA-mediated caspase knockdown was found to have significantly alleviated ACR-induced pyroptosis, the related protein expression was examined to further verify the key role of the NLRP3 inflammasome cascade (Fig. 6A and Fig. 7A). Compared with that of the control siRNA group, the NLRP3 inflammasome complex protein and downstream inflammatory factor expression was significantly increased in the ACR-exposed control siRNA group, whereas NLRP3 inflammasome complex protein expression, including NLRP3, cleaved caspase-1 and N-GSDMD, was significantly reduced following caspase-1 siRNA silencing (Fig. 6B-D). In addition, the release of IL-1β had decreased, suggesting that caspase-1 knockdown markedly decreased the ACR-induced NLRP3 inflammasome activation (Fig. 6E). Moreover, caspase-3 siRNA could significantly reduce the protein expressions of cleaved caspase-8, caspase-3 and N-GSDME, while also inhibiting IL-1β release (Fig. 7B-E). Comparative analysis of the IL-1β variation trend subsequent to caspase-1 knockdown and caspase-3 knockdown revealed that caspase-1 exerted a substantially greater activating effect on IL-1β. Thus, these findings confirm that, in line with the LDH release results, the NLRP3-caspase 1-GSDMD-IL-1β signaling axis plays a primary role in ACR-induced pyroptosis.

Discussion

ACR is a typical environmental and food contaminant, which presents potential health hazards and, thus, has attracted increasing attention. The present study, based on in vitro experiments, demonstrated the pathological significance of neuroinflammatory responses in the neurotoxic effect of ACR in dopaminergic neurons. The results showed that both the canonical pyroptotic pathway (NLRP3 inflammasome-related) and alternative pyroptotic pathway (caspase-3/GSDME axis) contributed to ACR-induced neurotoxicity. Moreover, we also found that ACR-induced canonical pyroptotic pathway (NLRP3 inflammasome-related) occurred within 6 h of inflammasome activation, while alternative pyroptosis

(caspase-3/GSDME axis) in this study was delayed. Additionally, compared to the alternative pyroptotic pathway, the NLRP3 inflammasome pathway was found to play a more significant role in ACR-induced pyroptosis through specific chemical inhibitor and small interfering RNA knockdown verification.

The NLRP3 inflammasome has recently been identified as a critical signaling of exogenous chemically-induced pyroptosis. In recent studies of ACR-induced neurotoxicity, it was shown that the NLRP3 inflammasome level was up-regulated in the hippocampi of rats after oral ACR administration, further increasing the expression levels of pro-inflammatory cytokines, IL-1β, interleukin-6 and IL-18 [30]. Moreover, as the resident immune cells in the central nervous system, microglial activation has been widely discussed in terms of ACR-induced NLRP3 inflammasome activation, both in vitro and in vivo [15,19]. Furthermore, neurons represent the main executors of nerve impulses and, therefore, their damage could cause cognitive impairment and motor dysfunction [31]. In this study, it was found ACR could induce cellular ballooning and lytic cell death in neurons, resulting in the activation of the NLRP3 inflammasome pathway and inducing the significant release of LDH, IL-1β and IL-18. Considering the essential functioning of neurons and microglia, it is apparent that the neurotoxic effects of ACR are presented not only through the microglial-derived immune response, but also directly via changes to the immunity homeostasis of neurons.

Additionally, in this study, an alternative form of pyroptosis was observed in ACR-induced neurotoxicity. This was found to be distinct from the canonical pyroptosis following NLRP3 inflammasome activation, due to their different occurrence times and mechanisms. Our study found, for the first time, that the ACR-induced caspase-8/caspase-3/GSDME signaling pathway induced the release of LDH and cytokines like IL-1β and IL-18 in SH-SY5Y cells. It is worth noting that GSDME, as a member of the gasdermin family, is also involved in the process of induced cell death [32]. Unlike GSDMD, GSDME is cleaved mainly by activated caspase-3 to form active N-GSDME, resulting in the loss of plasma membrane integrity and inducing the alternative form of pyroptosis [29]. Together, these data indicate that ACR is able to induce both canonical NLRP3 pyroptosis and alternative pyroptosis in SH-SY5Y cells. Furthermore, the combined blockage of the executor (caspase-1 and caspase-3) in the related pathway can alleviate ACR-induced pyroptosis to some extent, thereby rescuing the cell from death, indicating that these two pathways are main signal axes involved in the ACR-induced pyroptosis of SH-SY5Y cells.

The precise activation relationship between the NLRP3 inflammasome pathway (canonical pyroptosis) and the caspase-8/caspase-3/GSDME signal pathway (the alternative pyroptosis) in ACR-induced neurotoxicity remains unknown. However, it has been ascertained that canonical pyroptosis and the alternative pyroptosis cannot activate simultaneously. Canonical pyroptosis usually occurs shortly after inflammasome activation, while the alternative pyroptosis is generally delayed. However, such caspase-3-mediated alternative pyroptotic cell death may still take place as an auxiliary mechanism to promote innate immune responses against infections. Consistent with the previous hypothesis, our data showed that the ACR-induced pyroptosis of SH-SY5Y cells occurred first by activating the NLRP3 inflammasome signal pathway, and only then by means of the caspase-8/caspase-3/GSDME signal pathway. In addition, this study endeavored to ascertain which of the pathways present in ACR-induced neurotoxicity played

the most significant role. Our results showed that the blockage of caspase-1 (by Ac-YVAD-CMK treatment or siRNA gene silencing) can more significantly reduce the release of LDH and IL-1β, thereby alleviating ACR-induced pyroptosis, in comparison with that in caspase-3 blockage. Thus, it is apparent that the NLRP3/caspase-1/GSDMD signaling axis plays a primary role in ACR-induced pyroptosis.

Conclusion

The major finding of this study is that ACR can induce both canonical pyroptosis and the alternative pyroptosis in SH-SY5Y cells, and that canonical pyroptosis (via the NLRP3/caspase-1/GSDMD/IL-1β signaling axis) plays a primary role in ACR-induced pyroptosis (Fig. 8). Moreover, the NLRP3 inflammasome cascade is activated first during ACR exposure and the activation of these two pathways is time-dependent. It is therefore likely that such pyroptosis activation may intensify the innate immunity of the host to combat ACR-induced neurotoxicity.

Nonetheless, further research is warranted to explore the mechanism in in vivo relevance in an appropriate animal model. Moreover, the mechanism by which the alternative pyroptosis is activated, as well as that which triggers a transition of GSDMD-dependent pyroptosis into GSDMD-independent pyroptosis, remain unknown. One hypothesis is that the release of proinflammatory factors, such as IL-1β, via canonical pyroptosis may induce robust inflammation. Moreover, since caspase-3 is the key role effector protein in both pyroptosis and apoptosis, further research is needed to explore whether, in addition to caspase-8, any other upstream caspase is involved in inducing caspase-3 activation and GSDME-mediated cell death. The potential contribution of the synergistic effects of pyroptosis and apoptosis to the ACR-induced neurological mechanism also warrant further investigation.

Abbreviations

ACR, Acrylamide;

ASC, Apoptosis-associated speck-like protein containing CARD;

Caspase-1, Cysteinyl aspartate specific proteinase 1;

Caspase-3, Cysteinyl aspartate specific proteinase 3;

DMSO, Dimethyl sulfoxide;

FBS, Fetal bovine serum;

GSDMD, Gasdermin D;

GSDME, Gasdermin E;

GSH, Glutathione;

IL-1β, Interleukin-1β;

IL-18, Interleukin-18;

LDH, Lactate dehydrogenase;

MDA, Malondialdehyde;

MEM, Minimum Essential Medium;

MTT, 3-(4, 5-dimethyl-2-thiazolyl)-2, 5-diphenyl-2-H-tetrazolium bromide;

NAC, N-Acetyl-L-cysteine;

NLRP3, NOD-like receptor protein 3;

ROS, Reactive oxygen species;

TNF-α, Tumor necrosis factor-α.

Declarations

Author Contributions

Zhao Mengyao: Conceptualization, Methodology, Original draft preparation, Writing - Review & Editing, Project administration, Funding acquisition.

Zhang Boya: Investigation, Writing - Review & Editing.

Deng Linlin: Validation, Visualization.

Zhao Liming: Funding acquisition, Project administration, Supervision.

All authors read and approved the final manuscript.

Funding

This work was supported by the National Natural Science Foundation for Young Scientists of China (No. 31801668), the Shanghai PuJiang Program (18J1401900), the Shanghai Frontiers Science Center of Optogenetic Techniques for Cell Metabolism (Shanghai Municipal Education Commission).

Data Availability

All data in the current study are available from the corresponding authors on reasonable request.

Declarations

Ethics approval: Not applicable

Consent to Participate: Not applicable

Consent to publish: Not applicable

Competing Interests: The authors declare no competing interests.

Acknowledgments

This project was financially supported by the National Natural Science Foundation for Young Scientists of China (No. 31801668), the Shanghai PuJiang Program (18J1401900), the Shanghai Frontiers Science Center of Optogenetic Techniques for Cell Metabolism (Shanghai Municipal Education Commission)

References

1. Exon JH (2006) A review of the toxicology of acrylamide. J Toxicol Environ Health B Crit Rev 9 (5):397-412. doi:10.1080/10937400600681430
2. Busova M, Bencko V, Veszelits Lakticova K, Holcatova I, Vargova M (2020) Risk of exposure to acrylamide. Cent Eur J Public Health 28 Suppl:S43-S46. doi:10.21101/cejph.a6177
3. Uthra C, Shrivastava S, Jaswal A, Sinha N, Reshi MS, Shukla S (2017) Therapeutic potential of quercetin against acrylamide induced toxicity in rats. Biomed Pharmacother 86:705-714. doi:10.1016/j.biopha.2016.12.065
4. An L, Li G, Si J, Zhang C, Han X, Wang S, Jiang L, Xie K (2016) Acrylamide Retards the Slow Axonal Transport of Neurofilaments in Rat Cultured Dorsal Root Ganglia Neurons and the Corresponding Mechanisms. Neurochem Res 41 (5):1000-1009. doi:10.1007/s11064-015-1782-z
5. Mohr S, Stamler JS, Brüne B (1994) Mechanism of covalent modification of glyceraldehyde-3-phosphate dehydrogenase at its active site thiol by nitric oxide, peroxynitrite and related nitrosating agents. FEBS Letters 348 (3):223-227. doi:10.1016/0014-5793(94)00596-6
6. Murray SM, Waddell BM, Wu CW (2020) Neuron-specific toxicity of chronic acrylamide exposure in C. elegans. Neurotoxicol Teratol 77:106848. doi:10.1016/j.ntt.2019.106848
7. Liu Z, Song G, Zou C, Liu G, Wu W, Yuan T, Liu X (2015) Acrylamide induces mitochondrial dysfunction and apoptosis in BV-2 microglial cells. Free Radic Biol Med 84:42-53. doi:10.1016/j.freeradbiomed.2015.03.013
8. Lee JG, Wang YS, Chou CC (2014) Acrylamide-induced apoptosis in rat primary astrocytes and human astrocytoma cell lines. Toxicol In Vitro 28 (4):562-570. doi:10.1016/j.tiv.2014.01.005
9. Henn A, Lund S, Hedtjarn M, Schrattenholz A, Porzgen P, Leist M (2009) The suitability of BV2 cells as alternative model system for primary microglia cultures or for animal experiments examining brain inflammation. ALTEX 26 (2):83-94. doi:10.14573/altex.2009.2.83

10. Zhao M, Wang FSL, Hu XS, Chen F, Chan HM (2017) Effect of acrylamide-induced neurotoxicity in a primary astrocytes/microglial co-culture model. Toxicol In Vitro 39:119-125. doi:10.1016/j.tiv.2016.11.007
11. Zhao M, Wang P, Zhu Y, Liu X, Hu X, Chen F (2015) The chemoprotection of a blueberry anthocyanin extract against the acrylamide-induced oxidative stress in mitochondria: unequivocal evidence in mice liver. Food Funct 6 (9):3006-3012. doi:10.1039/c5fo00408j
12. Barber DS, LoPachin RM (2004) Proteomic analysis of acrylamide-protein adduct formation in rat brain synaptosomes. Toxicol Appl Pharmacol 201 (2):120-136. doi:10.1016/j.taap.2004.05.008
13. Santhanasabapathy R, Vasudevan S, Anupriya K, Pabitha R, Sudhandiran G (2015) Farnesol quells oxidative stress, reactive gliosis and inflammation during acrylamide-induced neurotoxicity: Behavioral and biochemical evidence. Neuroscience 308:212-227. doi:10.1016/j.neuroscience.2015.08.067
14. Yan D, Pan X, Yao J, Wang D, Wu X, Chen X, Shi N, Yan H (2019) MAPKs and NF-kappaB-mediated acrylamide-induced neuropathy in rat striatum and human neuroblastoma cells SY5Y. J Cell Biochem 120 (3):3898-3910. doi:10.1002/jcb.27671
15. Sui X, Yang J, Zhang G, Yuan X, Li W, Long J, Luo Y, Li Y, Wang Y (2020) NLRP3 inflammasome inhibition attenuates subacute neurotoxicity induced by acrylamide in vitro and in vivo. Toxicology 432:152392. doi:10.1016/j.tox.2020.152392
16. Hanamsagar R, Torres V, Kielian T (2011) Inflammasome activation and IL-1beta/IL-18 processing are influenced by distinct pathways in microglia. J Neurochem 119 (4):736-748. doi:10.1111/j.1471-4159.2011.07481.x
17. Afonina IS, Zhong Z, Karin M, Beyaert R (2017) Limiting inflammation-the negative regulation of NF-kappaB and the NLRP3 inflammasome. Nat Immunol 18 (8):861-869. doi:10.1038/ni.3772
18. Wu AG, Zhou XG, Qiao G, Yu L, Tang Y, Yan L, Qiu WQ, Pan R, Yu CL, Law BY, Qin DL, Wu JM (2021) Targeting microglial autophagic degradation in NLRP3 inflammasome-mediated neurodegenerative diseases. Ageing Res Rev 65:101202. doi:10.1016/j.arr.2020.101202
19. Liu Y, Zhang X, Yan D, Wang Y, Wang N, Liu Y, Tan A, Chen X, Yan H (2020) Chronic acrylamide exposure induced glia cell activation, NLRP3 infl-ammasome upregulation and cognitive impairment. Toxicol Appl Pharmacol 393:114949. doi:10.1016/j.taap.2020.114949
20. Zhao M, Deng L, Lu X, Fan L, Zhu Y, Zhao L (2022) The involvement of oxidative stress, neuronal lesions, neurotransmission impairment, and neuroinflammation in acrylamide-induced neurotoxicity in C57/BL6 mice. Environ Sci Pollut Res Int. doi:10.1007/s11356-021-18146-2
21. Peng D, Li J, Deng Y, Zhu X, Zhao L, Zhang Y, Li Z, Ou S, Li S, Jiang Y (2020) Sodium para-aminosalicylic acid inhibits manganese-induced NLRP3 inflammasome-dependent pyroptosis by inhibiting NF-kappaB pathway activation and oxidative stress. J Neuroinflammation 17 (1):343. doi:10.1186/s12974-020-02018-6
22. Wang Y, Yin B, Li D, Wang G, Han X, Sun X (2018) GSDME mediates caspase-3-dependent pyroptosis in gastric cancer. Biochem Biophys Res Commun 495 (1):1418-1425.

doi:10.1016/j.bbrc.2017.11.156

23. Xia W, Li Y, Wu M, Jin Q, Wang Q, Li S, Huang S, Zhang A, Zhang Y, Jia Z (2021) Gasdermin E deficiency attenuates acute kidney injury by inhibiting pyroptosis and inflammation. Cell Death Dis 12 (2):139. doi:10.1038/s41419-021-03431-2
24. Alrashidi H, Eaton S, Heales S (2021) Biochemical characterization of proliferative and differentiated SH-SY5Y cell line as a model for Parkinson's disease. Neurochem Int 145:105009. doi:10.1016/j.neuint.2021.105009
25. Deng L, Zhao M, Cui Y, Xia Q, Jiang L, Yin H, Zhao L (2021) Acrylamide induces intrinsic apoptosis and inhibits protective autophagy via the ROS mediated mitochondrial dysfunction pathway in U87-MG cells. Drug Chem Toxicol:1-12. doi:10.1080/01480545.2021.1979030
26. Wang Y, Gao W, Shi X, Ding J, Liu W, He H, Wang K, Shao F (2017) Chemotherapy drugs induce pyroptosis through caspase-3 cleavage of a gasdermin. Nature 547 (7661):99-103. doi:10.1038/nature22393
27. Pei P, Yao X, Jiang L, Qiu T, Wang N, Yang L, Gao N, Wang Z, Yang G, Liu X, Liu S, Jia X, Tao Y, Wei S, Sun X (2019) Inorganic arsenic induces pyroptosis and pancreatic beta cells dysfunction through stimulating the IRE1alpha/TNF-alpha pathway and protective effect of taurine. Food Chem Toxicol 125:392-402. doi:10.1016/j.fct.2019.01.015
28. Loboda A, Damulewicz M, Pyza E, Jozkowicz A, Dulak J (2016) Role of Nrf2/HO-1 system in development, oxidative stress response and diseases: an evolutionarily conserved mechanism. Cell Mol Life Sci 73 (17):3221-3247. doi:10.1007/s00018-016-2223-0
29. Shen X, Wang H, Weng C, Jiang H, Chen J (2021) Caspase 3/GSDME-dependent pyroptosis contributes to chemotherapy drug-induced nephrotoxicity. Cell Death Dis 12 (2):186. doi:10.1038/s41419-021-03458-5
30. Zong C, Hasegawa R, Urushitani M, Zhang L, Nagashima D, Sakurai T, Ichihara S, Ohsako S, Ichihara G (2019) Role of microglial activation and neuroinflammation in neurotoxicity of acrylamide in vivo and in vitro. Arch Toxicol 93 (7):2007-2019. doi:10.1007/s00204-019-02471-0
31. Xiao JW, Guo CL, Niu KL, Zhong-Sheng LI, Meng HL, Bin LI (2011) Effects of Schwan cells on damage and repair of motor neuron induced by acrylamide. J Journal of Toxicology 25(05):328-331. doi: 10.16421/j.cnki.1002-3127.2011.05.022
32. An H, Heo JS, Kim P, Lian Z, Lee S, Park J, Hong E, Pang K, Park Y, Ooshima A, Lee J, Son M, Park H, Wu Z, Park KS, Kim SJ, Bae I, Yang KM (2021) Tetraarsenic hexoxide enhances generation of mitochondrial ROS to promote pyroptosis by inducing the activation of caspase-3/GSDME in triple-negative breast cancer cells. Cell Death Dis 12 (2):159. doi:10.1038/s41419-021-03454-9

Figures

Figure 1

ACR induced pyroptosis and oxidative injury in SH-SY5Y cells

Figure 2

ACR induced pyroptosis-related proteins expression in SH-SY5Y cells

Figure 3

The phenotype of SH-SY5Y cells after different time ACR exposure

Figure 4

ACR sequentially activated proteins in canonical pyroptotic pathway and alternative pyroptotic pathway

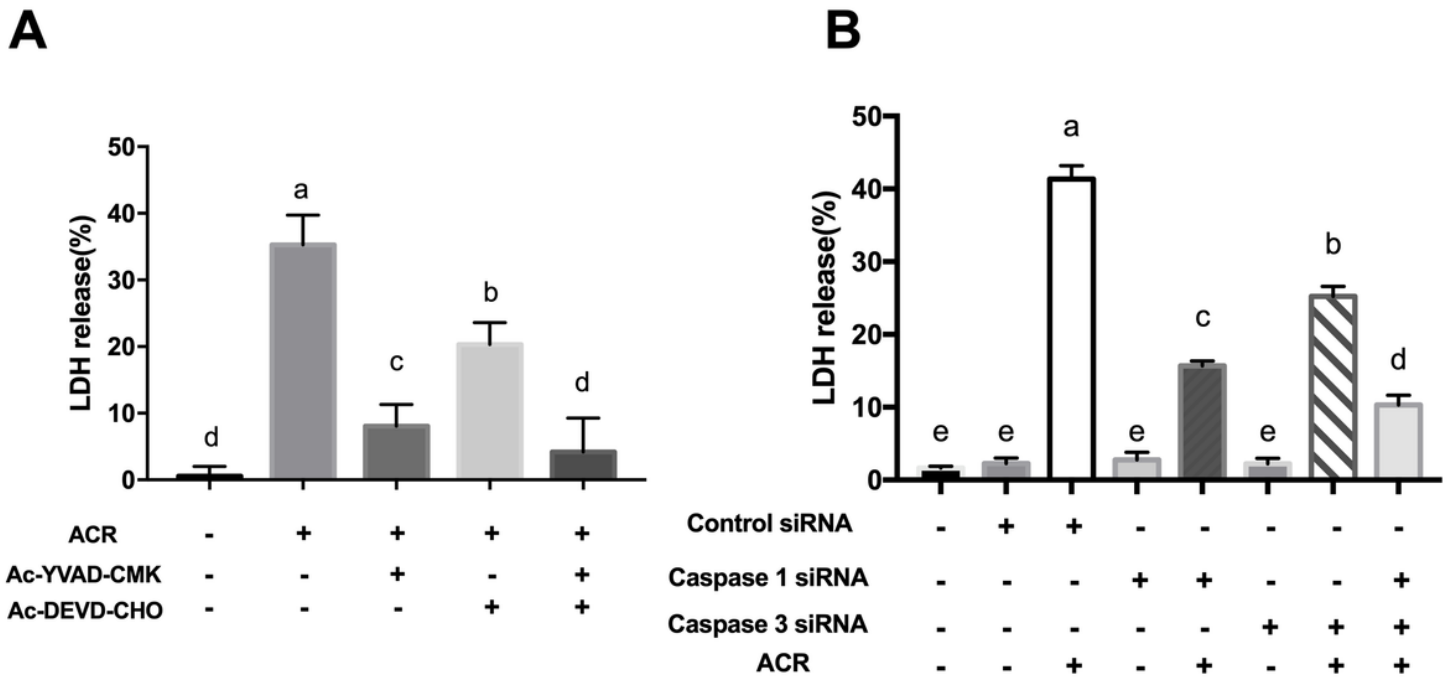

Figure 5

ACR-induced pyroptosis were inhibited after caspase inhibition treatment in the SH-SY5Y cells

Figure 6

Caspase-1 siRNA silencing attenuated ACR-induced pyroptosis by reducing protein expression in NLRP3 inflammasome pathway

Figure 7

ACR-induced alternative pyroptotic related protein expression after caspase 3 siRNA silencing

Figure 8

The potential mechanism of ACR induced pyroptosis

Supplementary Files

This is a list of supplementary files associated with this preprint. Click to download.

- Supplementaryfile1.docx